치의과학 박사학위논문

Non-Inferiority Evaluation of Osteoconductivity and Physical Properties of Deproteinized Bovine Bone Mineral (DBBM)

탈단백 우골 (DBBM)의 골전도성 및
물리적 성질에 대한 비열등성 평가

2022년 8월

서울대학교 대학원
치의과학과 치과생체재료과학 전공
이 다 정

Non-Inferiority Evaluation of Osteoconductivity and Physical Properties of Deproteinized Bovine Bone Mineral (DBBM)

지도교수 안 진 수

이 논문을 치의과학 박사학위논문으로 제출함
2022년 5월

서울대학교 대학원
치의과학과 치과생체재료과학 전공
이 다 정

이다정의 박사학위논문을 인준함
2022년 7월

위 원 장	임 범 순	(인)
부위원장	안 진 수	(인)
위 원	이 상 훈	(인)
위 원	김 성 태	(인)
위 원	오 승 한	(인)

Abstract

Non-Inferiority Evaluation of Osteoconductivity and Physical Properties of Deproteinized Bovine Bone Mineral (DBBM)

Program in Dental Biomaterials Science, Department of Dental Science, Graduate School, Seoul National University

(Directed by Professor Jin-Soo Ahn, *D.D.S., M.S.D., Ph.D.*)

Dajung Lee

The aim of this study is to compare physical properties and to evaluate osteoconductivity after guided bone regeneration (GBR) using two deproteinized bovine mineral (DBBM). The sample of study was comprised for DBBM (DBBM 1; InterOss, DBBM 2; A-Oss). The physical properties were preceded by scanning electron microscopy, X-ray diffraction, Fourier-transform infrared spectroscopy analysis.

In a subsequent in vivo test, osteoconductivity was evaluated in 6 beagle dogs. Alveolar defects in the mandible were created and filled with two DBBMs that were manufactured using a similar process and were randomly allocated. All of the flaws were covered with collagen membrane and had a 12-week healing time. Histological, histomorphometric, and linear/volumetric studies were done after the sacrifice process.

The result of physical properties was similar between DBBM 1 and DBBM 2. In the in vivo test results, no complications occurred during the healing period in both groups. Both DBBM groups had similar histology results, indicating that bone remodeling and new bone formation had occurred. Newly created vital bone surrounds residual bone particles. In histomorphometric study, the ratio of vital bone and residual bone substitutes area for DBBM 2 (38.18 %; 3.47 %) was larger than that of DBBM 1 (33.74 %; 3.41 %), but there was no statistically significant difference. In linear and volumetric study uses microcomputed tomography scanning and digital images of dental cast, there was no statistically significant difference between the two groups.

The two DBBMs had similar osteoconductivity due to their low crystalline carbonate apatite structures. The study shows that DBBM 1 is non-inferior to DBBM 2 in terms of osteoconductivity and volume maintenance.

Keyword : Bone Substitute; Xenograft; Physical Properties; Osteoconductivity; Apatite; Non-Inferiority

Student Number : 2019-30547

Table of Contents

Figure and Table Captions

1. Introduction

The alveolar ridge changes after tooth extraction due to resorption of the bundle bone. The horizontal dimensions change (29–63%) is more prominent than the vertical dimensional change (11–22%) during the healing period [1]. Different parts of bundle bone, in particular, lead to increased resorption of the buccal bone area [2]. Alveolar bone loss might potentially be the result of continuous mechanical overloading. The ideal position for implant placement would be hampered by bone resorption. The one- and two-wall types of bone defects, in particular, are difficult for bone grafting and subsequent implant placement [3].

Guided bone regeneration (GBR), which uses bone graft material around a bony wall to compensate for these dimensional changes, has been introduced to compensate for these changes. Several studies on GBR have been conducted using a variety of materials. GBR (vertical and horizontal alveolar ridge augmentation) was suggested by Urban I et al. as a standard choice for providing bone support for dental implants [4]. Bone graft materials have essential features such as osteogenesis, osteoinduction, and osteoconduction. Despite these properties, autogenous bone has the disadvantage of causing patient discomfort throughout the acquisition process [5]. In clinical use, demineralized freeze-dried bone allograft (DFDBA) has the drawbacks of bone resorption and inflammation as an alternative method [6]. An autogenous bone graft is superior to other bone substitutes such as DFDBA, tricalciumphosphate, and hydroxyapatite in the initial healing phase, according to Buser et al. [7]. Synthetic bone graft materials and bovine and

porcine-based xenografts have also been introduced. Xenografts from mammal species have been recommended as bone substitutes due to its comparable histologic shape and collagen composition [8]. Organic components are removed from bones using thermochemical methods. It could be possible to make a mineral scaffold with residual collagen [9].

In clinical practice, deproteinized bovine bone mineral (DBBM) is widely used. It is a safe and biocompatible material with osteoconductive abilities that contains 100% inorganic bovine bone [10]. To minimize the immunological reaction, DBBM is composed of porous particles (particle size: 0.25 – 2 mm) and is made by eliminating the organic components at high temperatures. After the organic components are removed, the porosity, chemical composition, and crystallite of DBBM are similar to that of human cancellous bone. DBBM also has a large surface area and promotes the growth of blood vessels and osteogenic cells, which leads to increased bone formation [11, 12]. However, crystallinity and surface irregularity increase if the temperature is too high beyond the range of 195 ℃ to 650 ℃ for deproteinization, which may impact the slowing of resorption rates [13].

A previous study reported that DBBM particles functioned well over the 7 months healing period after grafting in extraction sockets [14]. Not only is DBBM used to recover the extraction socket, but it is also used to recover periodontal tissue. A decrease in probing depth and an increase in clinical attachment level were observed after 9 months of DBBM treatment of a single periodontal infrabony defect [15, 16]. In addition, Nevins et al. reported that 4–6 months after implant placement, DBBM could maintain the alveolar ridge and result in favorable soft tissue healing [15]. In a previous

study, 39% of newly formed bone was reported during DBBM sinus augmentation [17]. The number of comparative studies among DBBMs, however, is still insufficient. Manufacturers advertise that their bovine bone graft materials are similar to human bone in shape and composition. Clinicians, on the other hand, may find it difficult to know the specific shape and composition of DBBM on the market. This is due to the fact that, in most cases, only the manufacturer has information of its DBBM composition.

In this study, two DBBMs were used. The two DBBMs inform users that they are manufactured through low-temperature processing and an extremely low heating rate. Therefore, the purpose of this study is to identify the characteristics of the low-temperature process through the physical properties of commercial DBBMs of two different manufacturers, and to verify the actual preclinical results.

2. Materials and Methods

2.1. Physical properties analysis

The InterOss® (SigmaGraft Inc, Fullerton, USA) and A-Oss® (Osstem Implant Co., Seoul, Korea) bone grafting materials were purchased, used in this study, and their particle size was the same as 0.25 ~ 1.0 mm.

2.1.1. Microstructural analysis

The morphological characterization of bone surface were investigated using scanning electron microscopy (SEM; Apreo S, Thermo Fisher Scientific, Waltham, MA, USA). The average and standard deviation of the particle size of each DBBM were calculated using the images that were obtained at a magnification of ×100,000 by ImageJ® (National Institutes of Health, Bethesda, Maryland, USA).

2.1.2. Phase analysis

The crystalline phase composition of the samples was determined through X-ray diffraction (XRD; D8 ADVANCE, Bruker, Germany) operating at 40 kV and 40 mA with CuKα radiation to probe the 2θ range of 10°– 80°. The diffraction patterns were determined using the COD (Crystallography open database) and the PDF (Powder Diffraction File) pattern 09-0432.

2.1.3. Function analysis

Fourier-transform infrared spectroscopy (FT-IR; Spectrum 100, Perkin-Elmer, Waltham, MA, USA) was used for the chemical analysis of the bone

graft materials. A sample pellet was made by mixing 1 g of finely grounded DBBM with 300 g of potassium bromide powder (KBr). And then, with a part of the mixture, a final sample pellet with a diameter of 7 mm was made. With a total of 24 scans each run, the spectra were captured in the 4000 - 400 cm^{-1} region at a resolution of 4 cm^{-1}. FT-IR spectroscopy was performed in the absorption mode.

2.2. In vivo tests

The modified ARRIVE (Animal Research: Reporting of In Vivo Experiments) guidelines for preclinical research were used to design this in vivo preclinical study [18].

In this study, six adult beagle dogs (age 15 months; weight 10–15 kg) with completely erupted permanent teeth were used. The Institutional Animal Care and Use Committee approved the study design and protocols (CRONEX, Seoul, Korea, approval no. 202003001). Figure 1 presents the timeline of this study.

The sample size was calculated based on estimations from a previous study by Netto et al [19]. With 90% statistical power, the type I error was set at 0.05. G Power software 3.1 was used to do the calculations [20].

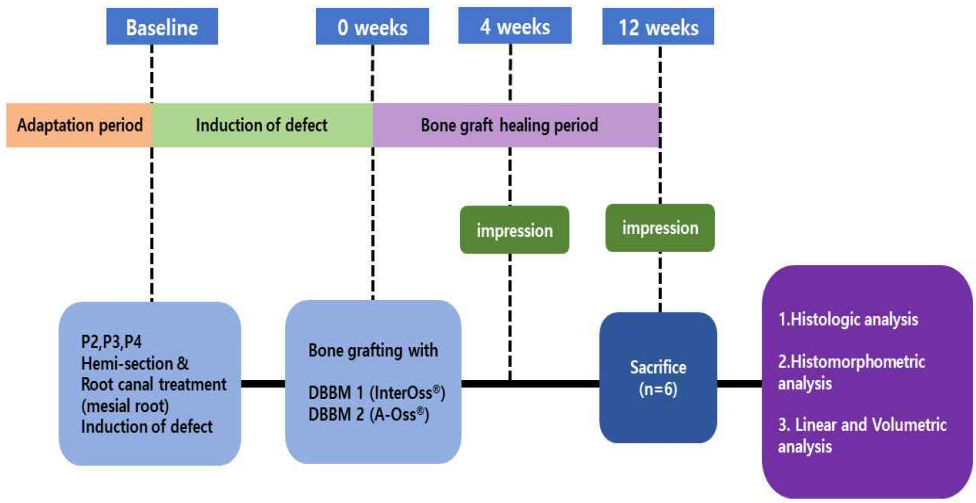

Figure 1. A flow diagram of study.

2.2.1. Surgery 1: induction of alveolar defect

The entire surgery was carried out under general anesthesia. A 1:1 mixture of 2 mL/10 kg zoletil 50 (tiletamine hydrochloride + zolazepam hydrochloride; Virbac S.A., France) and rompun was used to induce general anesthesia (xylazine hydrochloride; Bayer, Leverkusen, Germany). A 2:1 terrel solution (isoflurane; Piramal Critical Care Inc., Seoul, Korea) and oxygen were used to provide further respiratory anesthesia. Scaling was performed before surgery.

This investigation included the lower jaw of dogs. Lidocaine with 1:100,000 epinephrine was used to induce local anesthesia (Huons, Seongnam, Korea). Intracrevicular incision was performed on the surgical sites: mandibular second, third, and fourth premolar areas (P2, P3, and P4).

A rotating dental device was used to hemi-section three premolars (P2, P3,

and P4). Extraction forceps were used to remove the mesial roots of P2, P3, and P4. The P2, P3, and P4 distal roots were treated with root canal treatment, which included pulp removal with a 25-mm #15 K-file (MANI, Inc., Utsunomiya, Tochigi, Japan). Cold condensation was used to apply a gutta-percha master cone to the root canal. Around the master cone, additional accessory cones with root canal sealer (AH Plus; Dentsply, DeTrey GmbH, Konstanz, Germany) were placed. A dental sealing material was used to seal the treated root canal (IRM; Dentsply Sirona, Milford, DE, USA). According to previous studies [21, 22], the alveolar defect (5 × 5 × 5 mm) was surgically created on the extracted sites of each premolar (Figure 2A and B). The flap was sutured with a suture material (4-0 Vicryl®; Ethicon Inc., Somerville, NJ, USA) after induction of the alveolar defect.

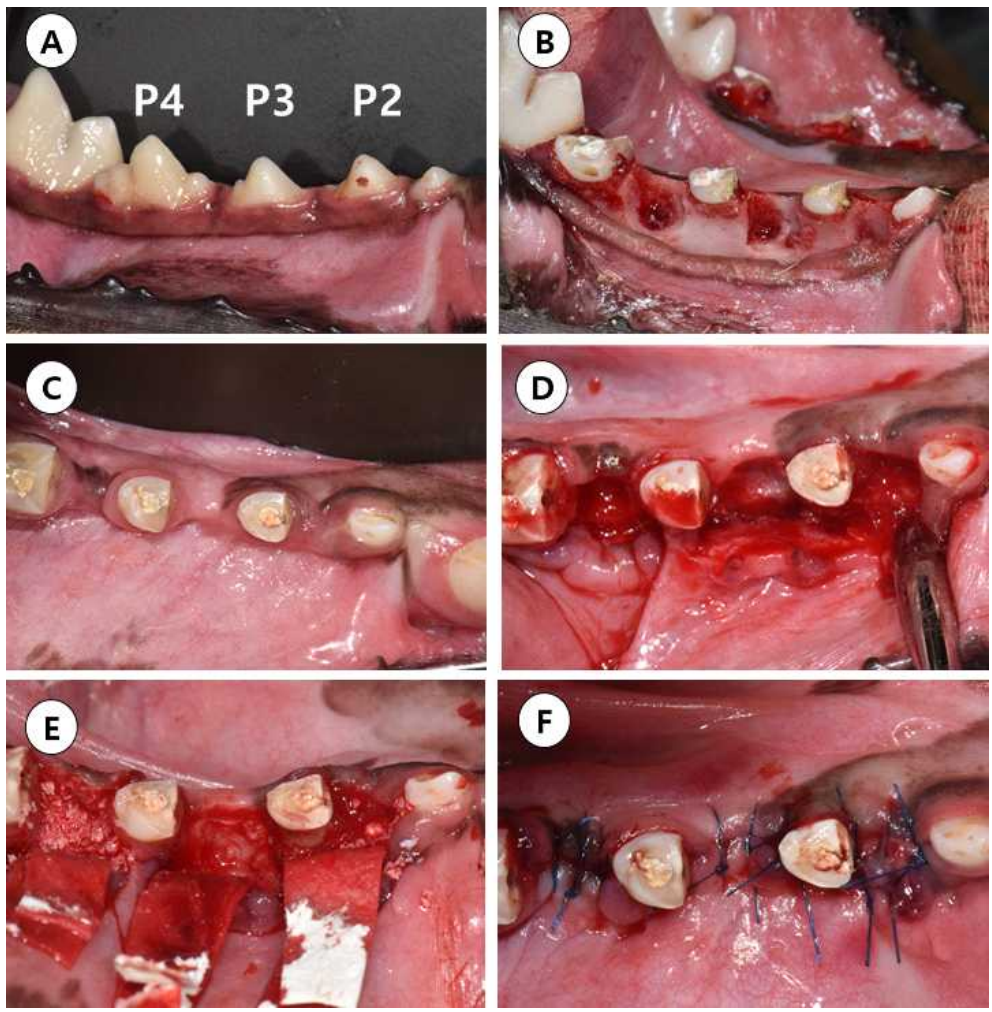

Figure 2. (A) Mandibular surgical sites. P2, second premolar; P3, third premolar; P4, fourth premolar area. (B) Hemi-section, defect creation (mesial extraction site) and endodontic treatment (distal root). (C) After 4weeks from defect creation. (D) Opened flap. (E) Bone graft material and resorbable membrane application. (F) Suture.

2.2.2. Surgery 2: guided bone regeneration 4 weeks after alveolar defect induction

GBR was conducted 4 weeks after the alveolar defect was created. On both lower sides of the alveolar bony defects, bone substitutes and resorbable membranes were divided into two groups.

- DBBM 1 (*N*=12): InterOss®, SigmaGraft Inc., Fullerton, USA
- DBBM 2 (*N*=12): A-Oss®, Osstem Implant Co., Seoul, Korea
- Collagen membrane: Bio-Gide®, Geistlich, Wolhusen, Switzerland

The same suture material was used to suture the open flap as in surgery 1. After the surgery, the dogs were given 0.2 mL/kg antibiotics (KOMI Biotril 100 Injection®; enrofloxacine, Komipharm Co. Ltd., Siheung-si, Korea) and 0.4 mg/kg analgesics (Metacam®; Meloxicam, Labiana Life science, S.A., Spain) for 3 days. After ten days, the sutures were removed. Chemical plaque control was used with 0.2% chlorhexidine during the healing period (Hexamedine; Bukwang Pharmaceutical, Seoul, Korea). The dogs were sacrificed using 1 mL of succipharm (suxamethonium chloride hydrate 50 mg; Komipharm Co. Ltd, Siheung-si, Korea) 12 weeks after surgery, and the experimental sites were obtained and fixed in 10% buffered formalin (Figure 2C-F).

2.2.3. Histological and histomorphometric analysis

Acrylic resin was used to embed the cross-sectioned specimens (Technovit 7200 VLC, Heraeus Kulzer, Wehrheim, Germany). Each specimen was cut to a thickness of 45 μm. Each specimen was stained using the Goldner trichrome method. The digitalization was done using a digital scanner (Pannoramic 250 Flash III, 3D HISTECH, Budapest, Hungary).

For histological and histomorphometric analyses, two image analysis softwares were used: Case Viewer® (3DHISTECH Kft., Budapest, Hungary) and ImageJ® (National Institutes of Health, Bethesda, Maryland, USA). On the histological image, a region of interest (ROI: 5 × 5 mm defect area) was defined. The relative composition of the total augmented area (%) with respect to vital bone area (VBA), residual bone substitutes area (RBA), fibrovascular tissue area (FVA), and bone marrow was evaluated in each histologic specimen of both experiments to assess the quality of the grafted area (Figure 3).

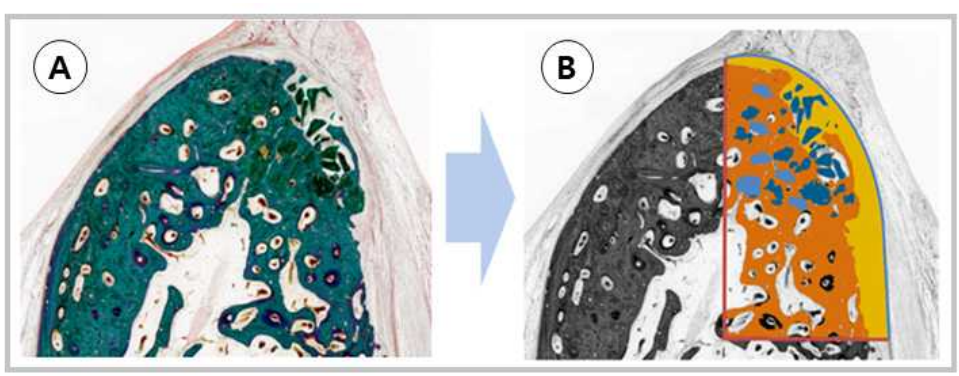

Figure 3. Histological and histomorphometric analyses: (A) Part of the stained histological image, (B) Identification of defined total augmented area and VBA, RBA, FVA, and bone marrow.

2.2.4. Microcomputed tomography scanning

The fixed block specimens were analyzed using microcomputed tomography (Bruker-microCT; SkyScan 1173, Kontich, Belgium) with a resolution of 24.9 μm (achieved using the scanner at 130 kV and 60 μA). To create three-dimensional (3D) shapes, the cross-sectioned data was reconstructed using NRecon and Dataviewer (Bruker-microCT, Kontich, Belgium) software. The total volume of the augmented area (ROI: 5 × 5 × 5 mm) was calculated using the CTAn software (Bruker-microCT, Kontich, Belgium) (Figure 4).

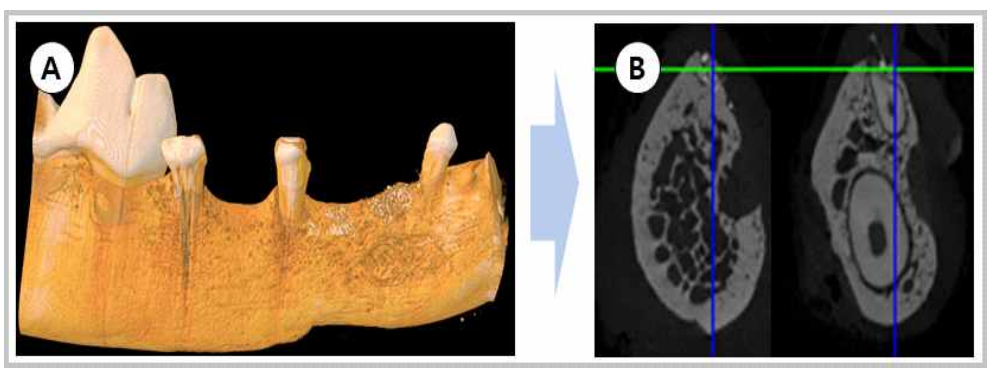

Figure 4. Microcomputed tomography scanning: (A) Scanned specimen, (B) Cross-sectioned data.

2.2.5. Linear and volumetric analysis

Dental impressions were obtained twice (at 1 month, and 3 months post-surgery) using impression materials (Aquasil Ultra LV® and Aquasil Ultra XLV® Dentsply DeTrey, Konstanz, Germany) and individual trays made by a 3D printer. Dental casts were poured out of dental stone (GC

Fujirock® type 4; GC Corporation, Tokyo, Japan) and digitized using a dental scanner (ZEISS COMET 5M, Oberkochen, Germany). The scanned STL file is superimposed on the basis of static points (non-moving reference point: canine and first molar) using a 3D metrology software (Geomagic Design X and Control X, 3D SYSTEMS, SC, USA). The volumetric and linear measurements were performed in the overlapping state (Figure 5, B).

Linear measurements in this study were performed according to the methods mentioned in previous studies [23, 24]. When the STL files were matched, a longitudinal slicing that divided the ridge into two equal area was made. Thereafter, the long axis of residual distal root (P2, P3, and P4) was selected as a vertical line on the sectional image. The perpendicular lines were drawn at the 0.5, 1.0, 1.5, and 2.0 mm from the most coronal area of the alveolar ridge. From the vertical line to the buccal contours, linear measurements were performed on each perpendicular line (0.5, 1.0, 1.5, and 2.0 mm) (Figure 5, C).

ROI (2.5 × 3.0 mm) was selected on the buccal area of each surgical sites (midcrestal line ~ buccal aspect) from the top view of the merged images. According to the ROI, a virtual block with the ROI dimensions was created including the surgical areas. Each volume of two periods (1- and 3-month later) overlapping with this virtual block was measured. The amount of change between these two periods was calculated by the method of a previous study [25] (Figure 5, D).

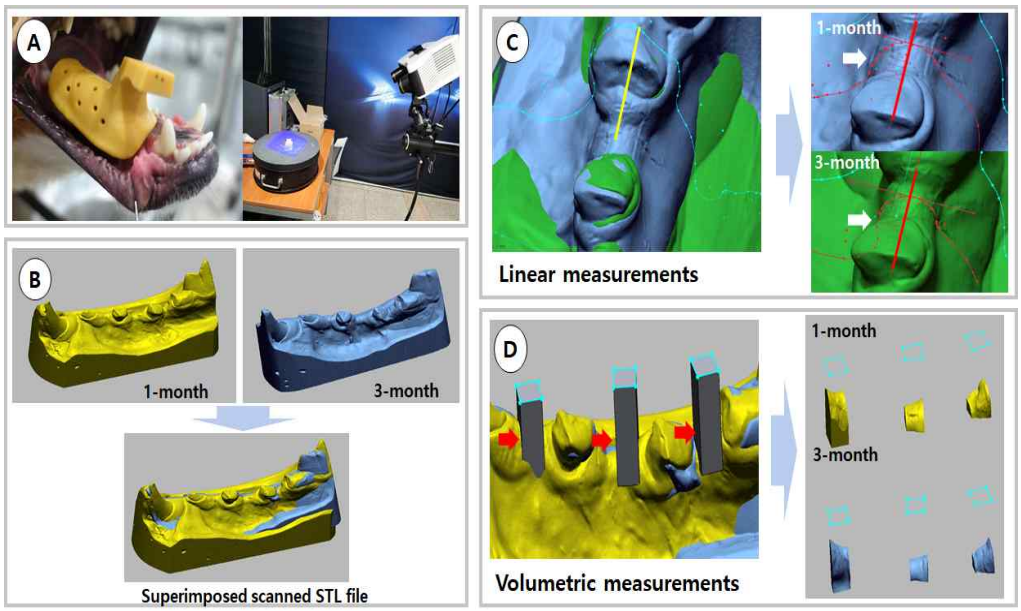

Figure 5. (A) Pre-fabricated individualized trays with 3D printer / Digitalized work of master cast with dental stone using dental scanner. (B) Scanned STL file (1- and 3- month), and superimposed file. (C) Linear measurement: long axis of residual distal root (yellow line) → application an imaginary line on the surgical site according to the long axis of residual distal root (red line) → setting perpendicular lines at 0.5, 1.0, 1.5, 2.0 mm from the alveolar crest → measuring the distance to the buccal surface (white arrows). (D) A virtual block with the region of interest (ROI: 2.5 × 3.0 mm) was created including the surgical areas (red arrows). Each volume of two periods overlapping with this virtual block was measured.

2.2.6. Statistical analysis

The software was used to perform statistical analysis (SPSS version 22.0, IBM Corp., Armonk, USA). The Shapiro–Wilk test was used to confirm the distribution's normality. If the parameters followed a normal distribution, independent t-tests or Mann–Whitney tests were performed between two groups (DBBM 1 and DBBM 2) for linear, volumetric, and histomorphometric analyses. A paired t-test or Wilcoxon signed rank test was used to assess differences between the periods (1 and 3 months later). The threshold for statistical significance was 5%.

3. Results

3.1. Physical properties analysis

3.1.1. Microstructural analysis

To investigate the surface morphology of both bone graft materials, the SEM analysis was conducted. Figure 6 shows that the morphology of both DBBMS was similar. Table 1 shows that the average particle size of the two DBBMs was also similar to DBBM 1 (0.15 ± 0.04 μm) and DBBM 2 (0.14 ± 0.04 μm).

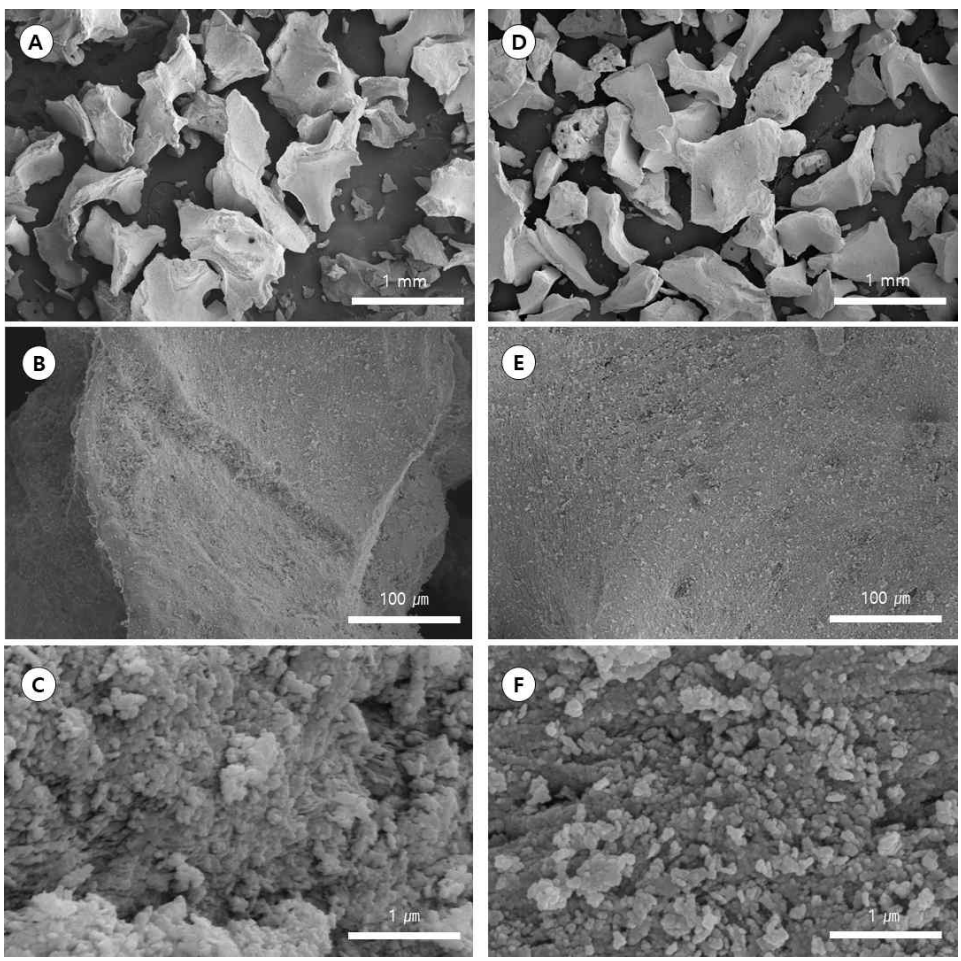

Figure 6. The SEM images of DBBMs: (A-C) DBBM 1, (D-F) DBBM 2.

Table 1. Comparison of mean particle size by SEM

Sample	Magnification	Mean particle size ± SD (μm)
DBBM 1	100,000 ×	0.15 ± 0.04
DBBM 2	100,000 ×	0.14 ± 0.04

3.1.2. Phase analysis

The crystallinity and phase identification of the bone graft materials were characterized through X-ray diffraction. Figure 7 demonstrates that the phase of the DBBMs was similar, with dominant peaks connected to hydroxyapatite (HAp). Compared to other bone graft materials, both DBBMs had a low degree of crystallinity [26].

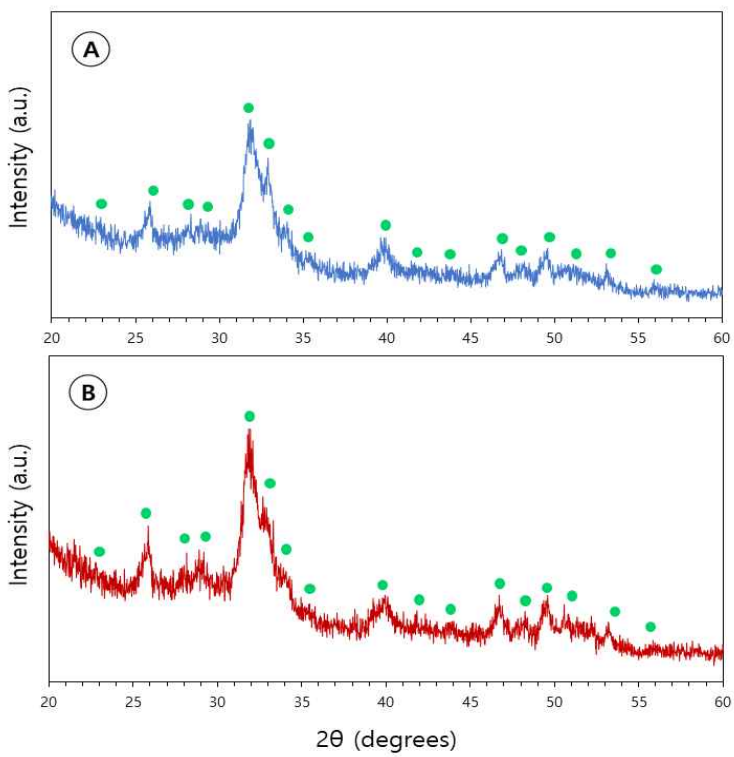

Figure 7. The XRD spectra of the DBBMs: (A) DBBM 1, (B) DBBM 2. The green dots mark the hydroxyapatite (HAp) peaks.

3.1.3. Function analysis

The chemical composition of the bone graft materials and their main functional groups were investigated through FT-IR analysis, as shown in Figure 8. The bands may be found in the wavelength ranges of 1454-1456 cm^{-1}, 1417 cm^{-1}, and 962 cm^{-1}, which correspond to the functional group (CO_3^{-2}) of the HAp. Additionally, the orthophosphates (PO_4^{3-}) were also seen at 1036 cm^{-1}, 603 cm^{-1}, 563 cm^{-1} and 472 cm^{-1}, as well as the stretching vibration of the hydroxyl groups (OH) at around 3568-3571 cm^{-1}.

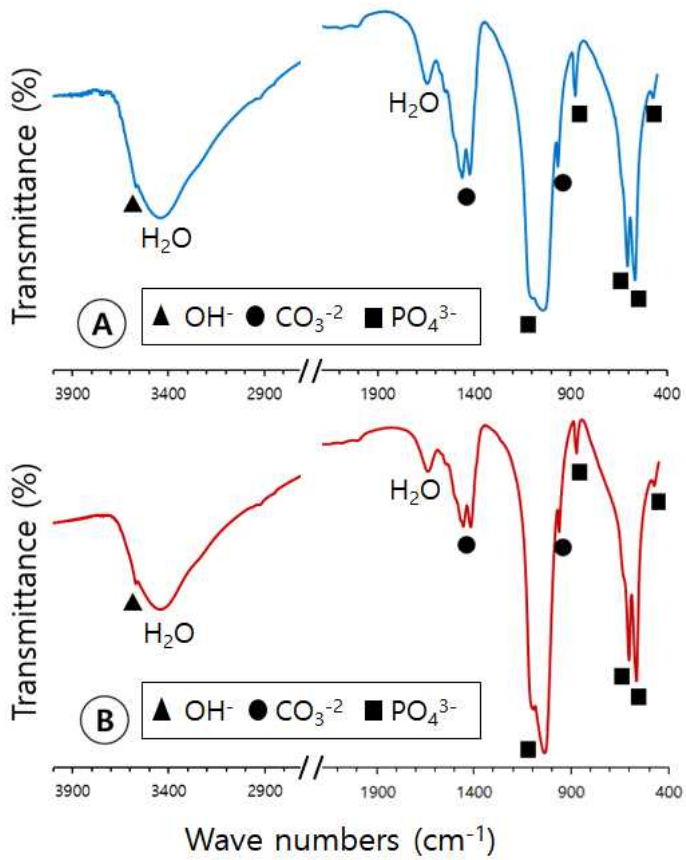

Figure 8. FT-IR spectra of DBBMs: (A) DBBM 1, (B) DBBM 2.

3.2. In vivo test

3.2.1. Histological and histomorphometric analysis

In histological analysis, no adverse inflammation associated with the bone graft material in all samples was observed. The resorbable membranes were well positioned over the entire ROI area (5 × 5 mm; defect area on histological image). In both groups, the bone remodeling was occurred and new bone was formed from the basal bone. Newly formed mature bone was observed between the particles. It is difficult to distinguish the new bone from the basal bone through the histologic images. Therefore, it is marked as ‘vital bone’. The dome-shaped augmented area was well maintained and residual bone graft particles were also maintained in both groups. (Figure 9). Histomorphometric analysis was performed to quantify the amount of residual bone graft material and the aspect of the retained volume. As a result of evaluating the ratio of VBA, RBA, and FVA to the total amount of ROI (TA), VBA and RBA values in DBBM 2 (38.18%; 3.47%) was higher than those of DBBM 1 (33.74%; 3.41%). Higher values of FVA and Bone marrow of DBBM 1(23.31%; 39.54%) than those of DBBM 2 (19.68%; 38.66%) were presented in Table 2. There was no significant difference between two groups.

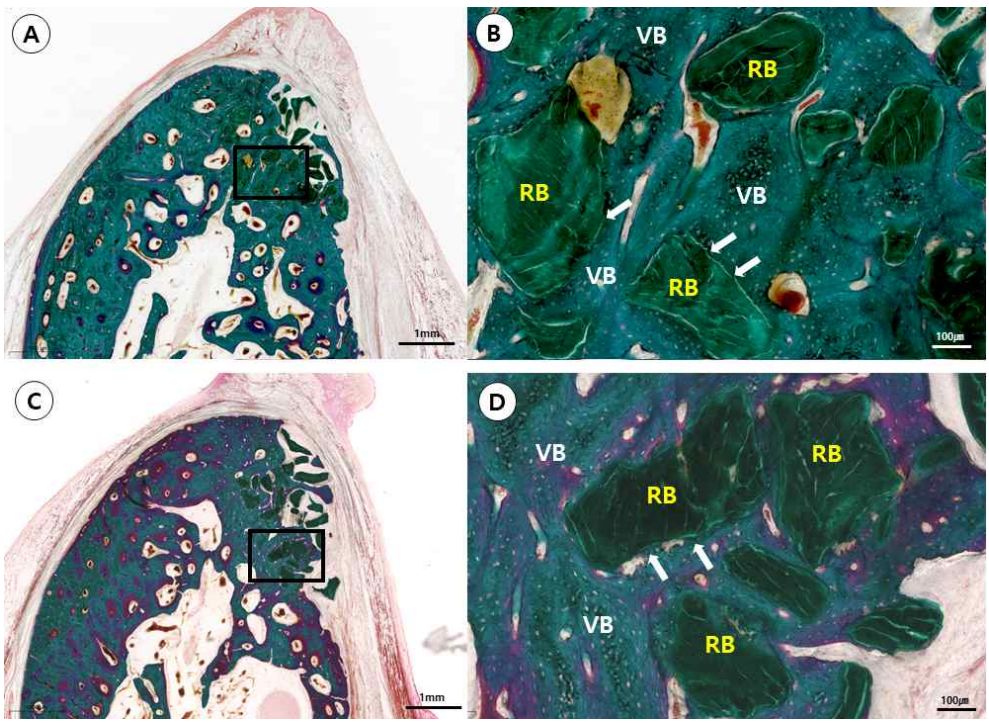

Figure 9. In the DBBM 1 and 2 groups, histological staining was performed. (A, B) DBBM 1. (C, D) DBBM 2. In two groups, the dome-shaped augmented area and residual bone graft particles were maintained. Between the particles in both groups, there was newly formed mature bone (white arrows). VB: vital bone. RB: Residual bone substitutes. The scale bar represents 1 mm (A, C) and 100 μm (B, D).

Table 2. Areal measurement of histomorphometric analysis (%)

	DBBM 1 Mean ± SD	DBBM 2 Mean ± SD
VBA/TA	33.74 ± 10.85	38.18 ± 9.99
RBA/TA	3.41 ± 3.97	3.47 ± 4.19
FVA/TA	23.31 ± 2.49	19.68 ± 2.46
Bone marrow/TA	39.54 ± 7.90	38.66 ± 9.55

Note: VBA, Vital bone area; RBA, Residual bone substitutes area; FVA, Fibro-vascular tissue area; TA, Total area; DBBM, Deproteinized bovine bone mineral.

3.2.2. Micro-computed tomography scanning

DBBM 1 occupies 40.44% and DBBM 2 accounts for 39.01% of the bone volume of the total ROI. Although DBBM 1 showed a slightly higher percentage of bone volume, the difference is not statistically significant (Table 3).

Table 3. Volumetric analysis of micro computed tomography and scanned image

	Bone volume ratio by micro CT (%)	Change between 1-month and 3-month later by scanned image of dental cast (%)
DBBM 1 Mean ± SD	40.44 ± 11.71	29.64 ± 17.83
DBBM 2 Mean ± SD	39.01 ± 6.63	29.42 ± 15.27

Note: DBBM; Deproteinized bovine bone mineral

3.2.3. Linear and volumetric analyses

The volume change between 1 month and 3 months of DBBM 1 (29.64 ± 17.83%) was slightly higher than that of DBBM 2 (29.42 ± 15.27%); however, this change is statistically insignificant (Table 3).

Linear measurements conducted at 1- and 3-month after surgery showed that the values significantly decreased after 3 months at all the measurement points, that is, 0.5, 1.0, 1.5, and 2.0 mm. The linear change between 1- and 3-month was smaller in DBBM 1 than that in DBBM 2. However, the intergroup difference was only significant at 1.5mm (Table 4).

Table 4. Linear change according to observation period after surgery

		1-month later	3-month later	Change between 1-month and 3-month later
DBBM 1	A (0.5 mm)	1.22 ± 0.29	1.06 ± 0.23 [A]	0.16 ± 0.18
Mean ± SD	B (1.0 mm)	1.79 ± 0.33	1.55 ± 0.18 [A]	0.23 ± 0.21
	C (1.5 mm)	2.29 ± 0.51	1.92 ± 0.32 [A]	0.37 ± 0.31 [a]
	D (2.0 mm)	2.71 ± 0.75	2.18 ± 0.54 [A]	0.52 ± 0.39
DBBM 2	A (0.5 mm)	1.24 ± 0.30	0.95 ± 0.18 [A]	0.29 ± 0.24
Mean ± SD	B (1.0 mm)	1.73 ± 0.26	1.48 ± 0.27 [A]	0.25 ± 0.34
	C (1.5 mm)	2.27 ± 0.53	1.70 ± 0.41 [A]	0.57 ± 0.37
	D (2.0 mm)	2.74 ± 0.74	2.09 ± 0.67 [A]	0.65 ± 0.41

Note: DBBM; Deproteinized bovine bone mineral

[A] Significantly different from one-month later (Statistical significance level was 5%, $p < 0.05$).

[a] Significantly different between two groups (Statistical significance level was 5%, $p < 0.05$).

4. Discussion

The results of both physical properties and in vivo experiments of two DBBMs were evaluated. In the physical properties test, SEM, XRD and FT-IR spectroscopy were used to compare the characteristic of two DBBMs.

Bone graft material of bovine origin have unlimited availability and excellent physical and structural similarities to human bones. However, residual can decrease biocompatibility and increase inflammation; hence, it is essential to remove organic components of ossicles to obtain bone mineral with both high purity and a natural spongy structure. The bone graft material from which organic components has been removed must have an appropriate crystal structure for osteoconductivity. Therefore, according to the SEM particle size analysis in this study, it can be seen that both groups have low crystallinity. In XRD, the peak width was relatively wide compared with other materials presented in previous studies, indicating that it has a low crystalline structure [26]. As a result of FT-IR analysis, it was confirmed that the bone graft material contains carbonic acid groups due to the low-temperature heat treatment process. Overall, it is evident that both groups are composed of low-crystalline carbonate apatite, which shares many of the physical characteristics as apatite found in bone.

In the in vivo test, two DBBMs were grafted into the alveolar bone defect in the mandible of beagles. The result of investigating sequential healing showed histologically significant difference in the area ratio of RBA. The linear volume change between 1 month and 3 months was small in

InterOss. However, there is not significant different between two DBBMs.

An in vivo test was performed on the beagle dog defect to verify the predictable bone tissue reaction, stable biocompatibility, and osteoconductivity. On the beagle dog defect, an in vivo test was performed to verify the predictable bone tissue reaction, stable biocompatibility, and safety. There was no inflammatory reaction throughout the three-month follow-up period. In the histological analysis, the results of investigating sequential healing were similar between two DBBMs for RBA, FVA, and bone marrow area. The VBA of DBBM 2 exceeds that of DBBM 1. In DBBM 1, the linear change between one and three months was less than in DBBM 2. However, in histologic and histomorphometric analyses, there were no significant differences between the two groups, with the exception of the linear C value in DBBM 1. Volume change was also almost the same in both DBBMs (DBBM 1: 29.64%, DBBM 2: 29.42%). DBBM has osteoconductive properties and provides a scaffold for vital bone formation. Khalid et al. reported that new bone formation using bovine bone was better than that with other synthetic bone materials (33% and 13–28%, respectively). In this study, the two DBBMs showed similar vital bone formation to a previous study (DBBM1: 34.25% and DBBM2: 38.59%, respectively) [27].

In a previous study, DBBMs were shown to have a slow rate of deterioration and a low capacity for bone regeneration [28]. By releasing bone morphogenic proteins, non-mineralized bone substitutes promote osteoblast differentiation. These non-mineralized bone materials, on the other hand, have inferior mechanical properties. The mineralized DBBM, on the other hand, has a better mechanical stability [29]. Bio-Oss®, a bovine bone

substitute, degraded at a significantly slower rate than other bone graft materials [30]. According to another study, Bio-Oss® resorption was not significant after 6 years [31]. Furthermore, previous study revealed that this delayed resorbed residual bone may be used as a scaffold to compensate for autogenous bone resorption in the clinic [32, 33]. The 3D structure of vital bone was seen using a micro CT scanner directed at the ROI to quantify the bone volume using DBBM 1 and 2 (40.4% and 39.0%, respectively). Most linear and volumetric parameters did not differ significantly between the two groups. It suggested that while both groups' overall bone volume was similar, the vital bone ratio in DBBM 2 was greater than in DBBM 1. It's possible that the structure and porosity (pore and interconnection size) of DBBMs have an impact on the findings of this study. In two groups, bone healing after grafting may occur through creeping substitution. In this study [29, 34], bone graft substitutes may begin to reconstruct through osteoclastic resorption and the generation of new vascular channels, followed by osteoblastic activity for new bone formation. However, more study involving immunohistochemical examination of osteoprotegerin, receptor activator of NF-kB (RANK), and its ligand RANKL is needed to identify the specific mechanism [35].

Depending on the component composition, architectural shape, and manufacturing process, the clinical outcome of DBBM may vary. As a result, several studies comparing the properties of DBBMs have been conducted. A previous study comparing sintered and non-sintered bovine bone blocks found that the sintered ones had much less bone resorption than the non-sintered ones [36]. On the dog model, Kim et al. analyzed two

particulate DBBMs (Bio-Oss® vs. InterOss®) and found that the materials had similar bone regeneration properties [37]. Bio-Oss®, BBP® (Oscotec, Seoul, Korea), and Osteograft® are three commercially available bone substitutes that Park described in detail (DIZG, Berlin, Germany). BBP® had a significant amount of residual protein, indicating that it might promote inflammation [38]. Previous studies has shown that the porosity of the particles, the surface area, and the purity of the material are all important factors in graft material maintenance [27, 39]. In previous studies, bovine bone substitutes were mostly made in one of two ways: at a low temperature (< 450°C) or at a high temperature (> 450°C). Large granules and high porosity characterize low-temperature bovine bone. It enables for improved osteoblast adhesion and protein structure persistence. High-temperature bovine bone, on the other hand, has a small porosity and small granules with a low possibility of residual proteins [40, 41]. Kübler et al. found that bovine bone had greater rates of osteoblast proliferation and differentiation than low-temperature bovine bone [41]. As a result, the osteoblasts were unable to adhere to the relatively flat surface of the granules. Both DBBM 1 and 2 were made in this study using a low-temperature process. Because the manufacturing processes of DBBM 1 and 2 were so similar, the products of the two DBBMs seemed to be similar.

In the histomorphometric and volumetric studies, scanned images were used. This technique is useful for determining alterations in soft and hard tissues in the oral cavity. Scanned images of the subject with the alginate impression are simple to acquire. This method had already been used in

study. Martin et al. used software to analyze the scanned cast model and evaluate the volumetric changes after implant placement [42]. Scanning casts has limitations, such as 1) errors during the impression procedure 2) limited accuracy of realizing soft tissue 3) discomfort, storage requirements. In this study, linear analysis was set from alveolar crest to 2.0 mm. The reason for this is that the soft tissue of the vestibule of the dogs may affect the impression procedure at a distance of more than 2.0 mm. It could be necessary to use for intra-oral scanner in the further studies.

This study has a few limitations. Since there are individual differences between animals and humans, it is necessary to evaluate the efficacy through long-term clinical trials. There was insufficient data for the histological changes over time. Further study for comparing to high-temperature bovine bone would be needed. In addition, this study lacks of comparison of Bio-Oss® which is the gold standard of DBBM. These limitations would be reinforced in following studies.

5. Conclusion

This study was carried out because there was a shortage of unbiased information, despite the fact that there are several local and international bone graft materials in use.

In this study, physical test and in vivo tests revealed that DBBM 1 and 2 had similar outcomes. It's possible that low-temperature processing of bovine bone materials will make them similar to human bone structure.

Subsequent in vivo test were conducted assuming that the osteoconductivity would be better due to the composition and structure of low-crystalline carbonate apatite. According to in vivo test results, DBBM 1 had a slower resorption rate than DBBM 2, and DBBM 1 had a smaller linear and volume change over the course of three months than DBBM 2. It means that at the same time, DBBM 2 may be replaced by more vital bone than DBBM 1. However, there were no significant differences between two groups.

In conclusion, the two DBBMs had a low crystalline carbonate apatite structure and thus had a similar osteoconductivity. The study demonstrate non-inferiority of DBBM 1 compared to DBBM 2 for maintenance and osteoconductivity.

References

1. Tan WL, Wong TL, Wong MC, Lang NP. A systematic review of post-extractional alveolar hard and soft tissue dimensional changes in humans. Clin Oral Implants Res 2012;23 Suppl 5:1-21.
2. Araújo MG, Lindhe J. Dimensional ridge alterations following tooth extraction. An experimental study in the dog. J Clin Periodontol 2005; 32:212-8.
3. Nevins ML, Camelo M, Rebaudi A, Lynch SE, Nevins M. Three-dimensional micro-computed tomographic evaluation of periodontal regeneration: A human report of intrabony defects treated with Bio-Oss collagen. Int J Periodontics Restorative Dent 2005;25:365–73.
4. Urban I, Caplanis N, Lozada JL. Simultaneous vertical guided bone regeneration and guided tissue regeneration in the posterior maxilla using recombinant human platelet-derived growth factor: A case report. J Oral Implantol 2009;35:251-6.
5. Kao ST, Scott DD. A review of bone substitutes. Oral Maxillofac Surg Clin North Am 2007;19:513-21.
6. Rosenberg E, Rose LF. Biologic and clinical consideration for autografts and allografts in periodontal regeneration therapy. Dent Clin North Am 1998;42:467-90.
7. Buser D, Hoffmann B, Bernard JP, Lussi A, Mettler D, Schenk RK. Evaluation of filling materials in membrane-protected bone defects. A comparative histomorphometric study in the mandible of miniature pigs. Clin Oral Implants Res 1998;9:137-50.
8. Schwartz Z, Weesner T, van Dijk S, Cochran DL, Mellonig JT, Lohmann

CH et al. Ability of deproteinized cancellous bovine bone to induce new bone formation. J Periodontol 2000;71:1258–69.

9. Esposito M, Felice P, Worthington HV. Interventions for replacing missing teeth: augmentation procedures of the maxillary sinus. Cochrane Database Syst Rev 2014;13:CD008397.

10. Panagiotou D, Karaca EÖ, İpçi ŞD, Çakar G, Olgaç V, Yılmaz S. Comparison of two different xenografts in bilateral sinus augmentation: radiographic and histologic findings. Quintessence Int 2015;46:611-9.

11. Peetz M. Characterization of xenogenic bone material (Appendix) to: Boyne PJ, ed. Osseous Reconstruction of the maxilla and the mandible: Surgical techniques using titanium mesh and bone mineral. Quintessence Books 1997; 87-93.

12. Rosen BV, Hobbs LW, Spector M. The ultrastructure of anorganic bovine bone and selected synthetic hydroxyapatite used as bone graft substitute materials. Biomaterials 2002;23:921-8.

13. Abdelmoneim D, Porter GC, Coates DE, Duncan WJ, Waddell JN, Hammer N, Li KC. The Effect of low-processing temperature on the physicochemical and mechanical properties of bovine hydroxyapatite bone substitutes. Materials (Basel) 2022;15(8)

14. Maiorana C, Poli PP, Deflorian M, Testori T, Mandelli F, Nagursky H, et al. Alveolar socket preservation with demineralised bovine bone mineral and a collagen matrix. J Periodontal Implant Sci 2017;47:194-210.

15. Nevins ML, Camelo M, Schupbach P, Kim DM, Camelo JM, Nevins M. Human histologic evaluation of mineralized collagen bone substitute and recombinant platelet-derived growth factor-BB to create bone for

implant placement in extraction socket defects at 4 and 6 months: a case series. Int J Periodontics Restorative Dent 2009;29:129-39.

16. Stavropoulos A, Karring T. Guided tissue regeneration combined with a deproteinized bovine bone mineral (Bio-Oss®) in the treatment of intrabony periodontal defects: 6-year results from a randomized-controlled clinical trial. J Clin Periodontol 2010;37:200-10.

17. Ferreira CE, Novaes AB, Haraszthy VI, Bittencourt M, Martinelli CB, Luczyszyn SM. A clinical study of 406 sinus augmentations with 100% anorganic bovine bone. J Periodontol 2009;80:1920-7.

18. Vignoletti F, Abrahamsson I. Quality of reporting of experimental research in implant dentistry. Critical aspects in design, outcome assessment and model validation. J Clin Periodontol 2012;39 Suppl 12: 6-27.

19. Netto HD, Olate S, Klüppel L, do Carmo AMR, Vásquez B, Albergaria- Barbosa J. Histometric analyses of cancellous and cortical interface in autogenous bone grafting. Int J Clin Exp Pathol 2013;6: 1532-7.

20. Faul F, Erdfelder E, Buchner A, Lang AG. Statistical power analyses using G* Power 3.1: Tests for correlation and regression analyses. Behavior research methods 2009;41:1149-60.

21. Shirakata Y, Imafuji T, Sena K, Shinohara Y, Nakamura T, Noguchi K. Periodontal tissue regeneration after low-intensity pulsed ultrasound stimulation with or without intra-marrow perforation in two-wall intra-bony defects - A pilot study in dogs. J Clinical Periodontol 2020;47: 54-63.

22. Lee J, Yun J, Kim K-H, Koo K-T, Seol Y-J, Lee Y-M. Periodontal

Regeneration Using Recombinant Human Bone Morphogenetic Protein-2 and a Bilayer Collagen Matrix. J Craniofac Surg 2020;31:1602-1607.

23. Di Raimondo R, Sanz-Esporrín J, Plá R, Sanz-Martín I, Luengo F, Vignoletti F, et al. Alveolar crest contour changes after guided bone regeneration using different biomaterials: An experimental in vivo investigation. Clin Oral Investig 2020;24:2351-2361.

24. Naenni N, Bienz SP, Benic GI, Jung RE, Hämmerle CH, Thoma DS. Volumetric and linear changes at dental implants following grafting with volume-stable three-dimensional collagen matrices or autogenous connective tissue grafts: 6-month data. Clin Oral Investig 2018;22:1185-1195.

25. Borges T, Fernandes D, Almeida B, Pereira M, Martins D, Azevedo L, et al. Correlation between alveolar bone morphology and volumetric dimensional changes in immediate maxillary implant placement: A 1-year prospective cohort study. J Periodontol 2020;91:1167-1176.

26. Lee J-H, Yi G-S, Lee J-W, Kim D-J. Physicochemical characterization of porcine bone-derived grafting material and comparison with bovine xenografts for dental applications. J Periodontal Implant Sci 2017;47: 388-401.

27. Al Ruhaimi KA. Bone graft substitutes: a comparative qualitative histologic review of current osteoconductive grafting materials. Int J Oral Maxillofac Implants 2001;16:105-14.

28. Kamadjaja DB, Sumarta NPM, Rizqiawan A. Stability of tissue augmented with deproteinized bovine bone mineral particles associated with implant placement in anterior maxilla. Case Rep Dent 2019;2019: 5431752.

29. Kamadjaja DB, Abidin ZZ, Diana R, Kharis I, Mira Sumarta NP, Amir MS, et al. In vivo analyses of osteogenic activity and bone regeneration capacity of demineralized freeze-dried bovine bone xenograft: A potential candidate for alveolar bone fillers. Int J Dent 2021;2021:1724374.

30. Piattelli M, Favero GA, Scarano A, Orsini G, Piattelli A. Bone reactions to anorganic bovine bone (Bio-Oss) used in sinus augmentation procedure: a histologic long-term report of 20 cases in humans. Int J Oral Maxillofac Implants 1999;14:835-40.

31. Schlegel AK, Donath K. BIO-OSS - a resorbable bone substitute? J Long Term Eff Med Implants 1998;8:201-9.

32. Maiorana C, Beretta M, Salina S, Santoro F. Reduction of autogenous bone graft resorption by means of bio-oss coverage: a prospective study. Int J Periodontics Restorative Dent 2005;25:19-25.

33. Hatano N, Shimizu Y, Ooya K. A clinical long-term radiographic evaluation of graft height changes after maxillary sinus floor augmentation with a 2:1 autogenous bone/xenograft mixture and simultaneous placement of dental implants. Clin Oral Implants Res 2004;15:339-45.

34. Wang W, Yeung KW. Bone grafts and biomaterials substitutes for bone defect repair: A review. Bioact Mater 2017;2:224-247.

35. Yamashita T, Takahashi N, Udagawa N. New roles of osteoblasts involved in osteoclast differentiation. World J Orthop 2012;3:175-81.

36. Gehrke SA, Mazón P, Del Fabbro M, Tumedei M, Aramburú Júnior J, Pérez-Díaz L, et al. Histological and histomorphometric analyses of two bovine bone blocks implanted in rabbit calvaria. Symmetry 2019;11:

641.

37. Kim DM, Hong H, Lin J, Nevins M. Evaluation of the bone-regenerating effects of two anorganic bovine bone grafts in a critical-sized alveolar ridge defect model. Int J Periodontics Restorative Dent 2017;37:234-244.

38. Park JW. Evaluation of deproteinized bovine bone mineral as a bone graft substitute; A comparative analysis of basic characteristics of three commercially available bone substitutes. J Periodontal Implant Sci 2005; 35:863-875.

39. Jensen SS, Aaboe M, Pinholt EM, Hjørting-Hansen E, Melsen F, Ruyter I. Tissue reaction and material characteristics of four bone substitutes. Int J Oral Maxillofac Implants 1996;11:55-66.

40. Lee DS, Pai Y, Chang S. Physicochemical characterization of InterOss® and Bio-Oss® anorganic bovine bone grafting material for oral surgery - A comparative study. Mater Chem Phys 2014;146:99-104.

41. Kübler A, Neugebauer J, Oh J-H, Scheer M, Zöller JE. Growth and proliferation of human osteoblasts on different bone graft substitutes an in vitro study. Implant Dentistry 2004;13:171-9.

42. Sanz Martin I, Benic GI, Hämmerle CH, Thoma DS. Prospective randomized controlled clinical study comparing two dental implant types: volumetric soft tissue changes at 1 year of loading. Clin Oral Implants Res 2016;27:406-11.

국문초록

탈단백 우골(DBBM)의 골전도성 및 물리적 성질에 대한 비열등성 평가

치의과학과 치과생체재료과학 전공

(지도교수 안 진 수)

이 다 정

본 연구의 목적은 두 개의 탈단백 우골(DBBM)을 사용하여 물리적 특성을 비교하고, 골유도재생술(GBR) 후의 골전도성을 평가하는 것이다. 연구 샘플은 DBBM(DBBM 1; InterOss, DBBM 2; A-Oss)으로 구성하였다. 주사전자현미경(SEM), X선 회절법(XRD), 푸리에 변환 적외선(FT-IR) 분광분석을 통해 물리적 특성을 분석하고, 후속적으로 생체 내 실험에서 6마리의 비글견에서 골전도성을 평가하였다. 하악 부위에 치조 결손부를 형성하고, 이를 각각 무작위로 할당된 2개의 DBBM으로 수복하였다. 모든 결손부는 콜라겐 차단막으로 덮고, 12주의 치유기간을 가졌다. 희생 절차 후에는 조직학적 및 조직형태학적 분석, 선형/체적 분석을 수행하였다.

두 개의 DBBM군 모두 유사한 조직학적 소견을 보였다. 골 재형성이 일어나 신생골이 형성되었으며, 잔존골 입자는 신생골로 둘러싸여 있었다. 조직형태학적 분석에서 DBBM 2 (38.18%; 3.47%)가 DBBM 1

(33.74%; 3.41%)보다 신생골과 잔존골 대체면적의 비율이 높았으나, 유의한 차이는 없었다. 또한 마이크로컴퓨터 단층촬영과 디지털화상을 이용한 치과모형의 선형분석과 체적분석에서도 두 그룹 간 통계적으로 유의한 차이는 없었다.

두 DBBM은 저결정성 탄산 아파타이트 구조로 인해 유사한 골전도성을 보였다. 따라서 본 연구에 따르면 DBBM 1은 골전도성 및 부피 유지 측면에서 DBBM 2에 비하여 열등하지 않다.

주요어 : 골 대체제; 이종골; 물리적 특성; 골전도성; 인회석; 비열등성

학 번 : 2019-30547